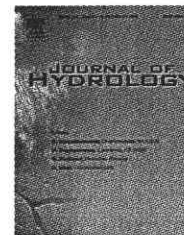


available at www.sciencedirect.com

journal homepage: www.elsevier.com/locate/jhydrol

Assessing the controls of the snow energy balance and water available for runoff in a rain-on-snow environment

Adam B. Mazurkiewicz ^a, David G. Callery ^a, Jeffrey J. McDonnell ^{a,b,*}

^a Oregon State University, Department of Forest Engineering, 204 Peavy Hall, Corvallis, OR 97331-5706, USA

^b Water Resources Section, Delft Technical University, Delft, The Netherlands

Received 3 April 2007; received in revised form 12 October 2007; accepted 29 December 2007

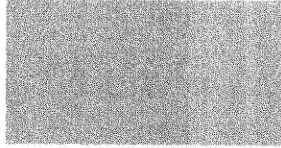
KEYWORDS

Snowmelt;
Rain-on-snow;
Snow hydrology;
Energy balance;
Pacific Northwest

Summary Rain-on-snow (ROS) melt production and its contribution to water available for runoff is poorly understood. In the Pacific Northwest (PNW) of the USA, ROS drives many runoff events with turbulent energy exchanges dominating the snow energy balance (EB). While previous experimental work in the PNW (most notably the H.J. Andrews Experimental Forest (HJA)) has quantified these energy balance components for a handful of ROS events, little is known about the EB components of snowmelt at HJA on an annual basis and how the relative importance of each component changes with different time periods of analysis. Beyond the few measured events at HJA and elsewhere in the PNW, there is still a lack of understanding of the dominant components of the EB during high-frequency ROS events and how much annual snowmelt is produced during ROS events. A physically based snow energy balance model (SNOBAL) was applied to data from three climate stations in the HJA to address these questions. Measurements of all required forcing data except incoming longwave radiation were made at each site. We employ the largest ROS dataset ever amassed with SNOBAL to use the model as a learning tool to characterize the snowmelt regime in the HJA. The results show that radiation dominated the melt energy balance over the period 1996–2003 while net turbulent energy exchanges were much lower than expected. Annual variability in EB components reflected duration of snowpack (snow covered period) – where later season snowpack resulted in higher radiation as percentage of the total EB. Radiation was the largest contributor to melt during ROS. These results question the general perception of turbulent energy exchange dominance of ROS and seasonal melt in the PNW. Overall, melt from ROS events was a small

* Corresponding author. Address: Oregon State University, Department of Forest Engineering, 204 Peavy Hall, Corvallis, OR 97331-5706, USA. Tel.: +1 541 737 8720; fax: +1 541 737 4316.

E-mail address: jeff.mcdonnel@oregonstate.edu (J.J. McDonnell).



percentage of annual melt – for the period 1996–2003 snow season, 80–90% of snowmelt comes from non-ROS days. These results prove the highly variable spatial and temporal controls on the snowmelt regime in the Pacific Northwest.

© 2008 Elsevier B.V. All rights reserved.

Introduction

Given the protracted rainfall regime of PNW winters and the hydrological importance of snowmelt during rainfall, the snowmelt in the PNW is often characterized as turbulent-exchange-dominated (Harr, 1981). Notwithstanding, very few experimental studies have actually focused on energy balance (EB) dynamics of melting snow in the PNW. The most extensive such work was conducted at the Willamette Basin Snow Laboratory (WBSL) in the Blue River Watershed during the period 1947–1952 (USACE, 1956). This project led to the development of general snowmelt equations and thermal budget indices. Berris and Harr (1987), working at the H.J. Andrews Experimental Forest (HJA) in the western Cascade Mountains of Oregon found that snowmelt in forested sites during ROS events were much lower than in open sites in the transient snow zone. Absence of a forest canopy resulted in continuous higher energy balance inputs to the snowpack creating a consistently isothermal snowpack. Marks et al. (1998) found 60–90% of snowmelt was driven by turbulent energy exchanges during one of the largest recorded ROS events in the region which occurred in February 1996. Van Heeswijk et al. (1996) showed that rainfall rates alone have little effect on the production of snowmelt. They reported that double the measured precipitation added only 0.1–0.5 mm snowmelt for the three events recorded, while adding 2 °C to the air temperature increased snowmelt by 0.7–5.8 mm. They concluded that the generation of snowmelt during ROS is most sensitive to wind speed in conjunction with vapor pressure and temperature gradients. Field experiments in the Austrian Alps have shown that transmission of rainfall through the snowpack can be exceptionally high during ROS events (up to 6 m/h when the snowpack becomes saturated) (Singh et al., 1997). These rapid percolation rates contribute to fast streamflow response but very little energy exchange for melt.

In spite of these detailed studies, there is little work that has quantified the EB components of snowmelt from event to seasonal to annual timescales. The percentage of annual snowmelt that is generated from ROS events vs. non-ROS event melt remains unclear. There is very limited data covering different times of the melt season and at different elevations to underpin the general notion of turbulent energy flux domination of the snow energy balance regime in the PNW. Hydrology studies to date have largely focused on streamflow data and often cite ROS events as the main driver of peak discharge in relation to forest management practices, e.g. “increases in ROS peak discharges after forest canopy removal are greater in basins with large snowpacks” (Jones and Swanson, 2001, p. 2365). While these studies provide a depiction of streamflow generation in the region, they do not decipher the snowmelt processes that create water available for runoff (WAR). Nevertheless, those studies which have focused on snowmelt processes have suggested that “energy budgets of snowmelt during rain-on-snow events show that the rela-

tively ‘warm’ rain provides little energy to melt snow. Rather, the primary source of energy to melt snow is the condensation of water vapor onto the snow pack” (Wondzell and King, 2003, p. 82). In their definitive study at the WBSL, the US Army Corp of Engineers stated that “no measures of solar radiation were obtained at WBSL because of its expected minor importance in the direct melt process at this location” (USACE, 1956, p. 209). In addition, there is also a general notion in the PNW that ground heat flux is not an influential component to the EB (Berris and Harr, 1987), that open sites produce more melt and WAR than forested sites (Marks et al., 1998; Berris and Harr, 1987), and that shallow snowpacks are most important for ROS where snowpacks melt out completely over the course of the single ROS event (Marks et al., 1998; Berris and Harr, 1987). To date, we have not had the datasets to test these generalizations. The few experimental studies in this and other regions have shown that turbulent energy exchanges are a large portion of the EB during ROS events and are a dominant driver of snowmelt.

In this paper we seek to improve our understanding of the snowmelt regime in the PNW using a physically based snow energy and mass balance model (SNOBAL) (Marks et al., 1998) as a learning tool (following the philosophy of Weiler and McDonnell, 2004; Loague et al., 2006). We simulate snow accumulation and melt to address some of the outstanding questions on the relative importance of the various energy balance components during ROS at different temporal scales and topographic settings. We use an eight year time series of snow accumulation and melt data from the HJA Long Term Ecological Research (LTER) site to better understand processes which are difficult to measure and quantify. With this work we go beyond the single-event, which has been the focus in this region to date (e.g. Berris and Harr, 1987; Marks et al., 1998, 2001, who focused on the 1996 event), and for the first time evaluate numerous ROS events of varied intensities to truly characterize the PNW snowmelt regime.

The main research questions explored in this paper are:

1. What are the EB components of snowmelt at HJA on an annual basis?
2. How does their relative importance change with different timescales?
3. What are the dominant components of the EB during high-frequency ROS events?
4. How much annual snowmelt comes from ROS events vs. non-ROS event melt?
5. How do energy balance components vary by site elevation, exposure, aspect?

Study site

The study sites are located within the HJA Experimental Forest, a part of the LTER program. The experimental forest

is located in the western Oregon Cascade Mountain Range, and encompasses the 62 km² drainage of Lookout Creek, a tributary to the Blue River in the McKenzie River Basin. Elevations in the HJA range from 800 to 2000 m. The Mediterranean climate produces approximately 80% of annual precipitation in the months between November and March, whereas summers are typically warm and dry (Fig. 1). Annual precipitation ranged from 1800 mm at low elevations to 3000 mm in the upper elevations during the study period. Above 1000 m, winter precipitation falls mainly as snow. The transient snow zone lies roughly between 500 and 1000 m. At these elevations, snow and rain are frequent in the winter months, with ROS events common. However, ROS events do occur at all elevations of the HJA during the winter. The elevation range and climate (Greenland, 1994) of the HJA is typical of the western Cascades in Oregon.

Data from three permanent climate stations were analyzed. These sites are located from the middle to upper elevations of the Lookout Creek basin: Central (1018 m) (CENMET), Vanilla Leaf (1273 m) (VANMET) and Upper Lookout (1294 m) (UPLMET) (Fig. 2). Each site has a similar array of sensors, which includes: air temperature, relative humidity, precipitation, incoming solar radiation, wind speed, ground temperature and snow pillows (Table 1). These sites have nearly complete data records for water years (WY) 1996–2003, providing a unique dataset to apply a physically based snow energy balance model.

Temperature and relative humidity were monitored using a HMP35C (Vaisala Inc., Woburn, MA) housed in a PVC radiation shield. Solar radiation was measured using a Kipp & Zonen model CM-6B pyranometer (spectral range: 0.3–2.8 μm). Wind speed was measured by a RM Young (Traverse City, MI) anemometer mounted at 10 m above ground. Soil temperature measured by Campbell Scientific Inc. (Logan, UT) thermistor probes at 20 cm was used for this investigation.

Cumulative precipitation gauges were located at each climate station. The VANMET precipitation gauge was a heated stand-alone with an alter wind shield. The CENMET precipitation gauge was located on the shelter house and utilizes the shelter's propane heating system. The primary precipitation gauge at UPLMET was a stand-alone gage with a Valdais wind shield. Steel snow pillows were located at each of the stations to measure snow water equivalence

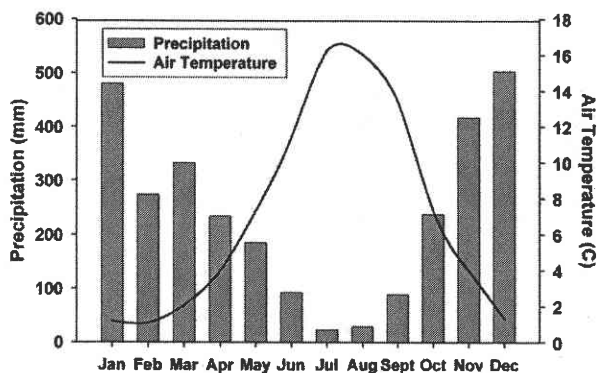


Figure 1 Climograph at Upper Lookout Meteorological station for years 1996–2003.

(SWE). Manual snow depth and SWE measurements were also taken periodically by field personnel.

Methods

Snow energy balance

The snow energy balance describes the amount of energy contributing towards snowmelt (Q_m). It is described as

$$Q_m = R_n + L_n + H + L_{ve} + G + M \quad (1)$$

where R_n is the net shortwave radiation, L_n is the net longwave radiation, H is the sensible heat exchange, L_{ve} is the latent heat of evaporation, G is the ground heat flux and M is the advected heat from precipitation. Net shortwave radiation (0.3–2.8 μm) is the total amount of solar radiation absorbed by the snowpack. Net longwave radiation is the amount of energy incident on the snow from the atmosphere and surrounding vegetation, less the amount of emitted thermal radiation from the snowpack. Sensible and latent heat are the turbulent exchanges and are highly dependent on wind speed. Sensible heat is the amount of convective heat transfer at the snow–air interface. Latent energy flux is a result of evaporation, condensation, or sublimation. Ground temperatures are often measured to be above 0 °C, therefore it is necessary to account for the energy conducted at the soil–snow interface. Differences in temperature between precipitation and the snowpack results in advected heat transfer. The energy available for melt is then added to the cold content, which is the amount of energy needed to bring the snowpack to isothermal conditions. If the energy available for melt is negative, then there is a net loss of energy from the snowpack.

SNOBAL

SNOBAL is a physically based snow energy and mass balance model, developed (Marks and Dozier, 1992) and described in detail by Marks et al. (1998) (Fig. 3). The model has been applied at a number of locations including central Canada (Link and Marks, 1999a), Turkey (Şensoy et al., 2006) and the Pacific Northwest (Marks et al., 1998; Marks and Winstral, 2002; Van Heeswijk et al., 1996). The spatially distributed version (ISNOBAL) has been successfully applied to the Boise River Basin (Garen and Marks, 2005), the Wasatch Range in Utah (Susong et al., 1999), the Boreal Ecosystem–Atmosphere Study (Link and Marks, 1999b), the California Sierra Nevada (Marks et al., 1999a), the Reynolds Creek Experimental Watershed (Winstral and Marks, 2002) and the central Washington Cascades (Mazurkiewicz, 2006). SNOBAL is a utility built in the Image Processing Workbench (IPW) (Frew, 1990; Marks et al., 1999b). The software operates in a UNIX environment with a command line interface. In addition to SNOBAL, IPW utilities were used to calculate thermal radiation, relative humidity to vapor pressure conversions and clear sky solar radiation (Marks et al., 1999b).

SNOBAL forcing data

The required forcing data for the model are net solar radiation, incoming thermal radiation, air temperature, precipi-

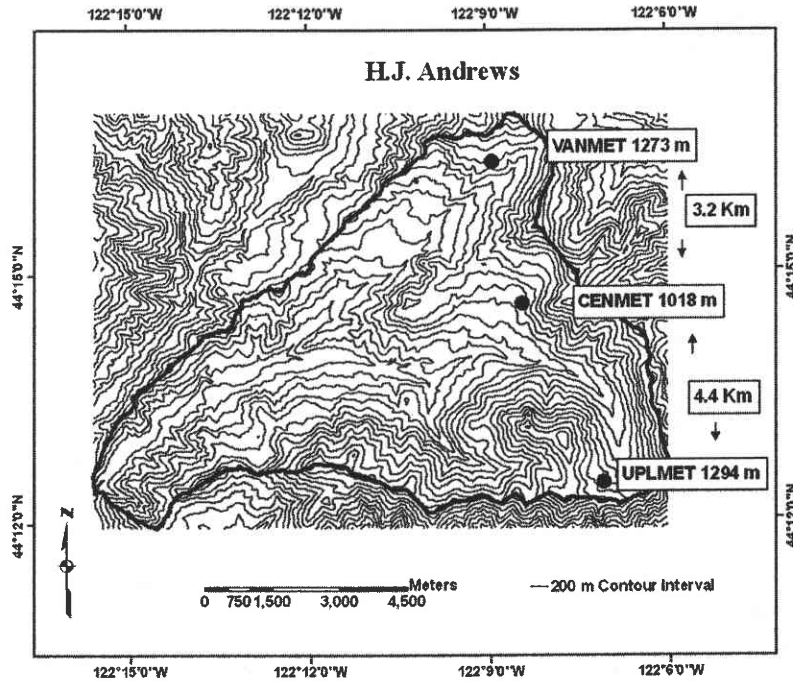


Figure 2 The H.J. Andrews Experimental Forest watershed, Western Oregon USA.

Table 1 Meteorological measurements

Parameter	Sensor	Sampling interval	Precision	Instrument height (above soil surface)
Wind speed	RM Young 05103 sensor	15 min	0.25 m/s	10 m
Air temperature	Campbell Model HMP35C	15 min	0.1 °C	450 cm
Relative humidity	Campbell Model HMP35C	15 min	0.1 °C	450 cm
Shortwave radiation	Kipp & Zonen CM-6B	15 min	0.05 langley	450–800 cm
Soil temperature	Campbell 107	15 min	0.1 °C	20 cm depth
Precipitation	Stand alone gauge	15 min	0.254 mm	

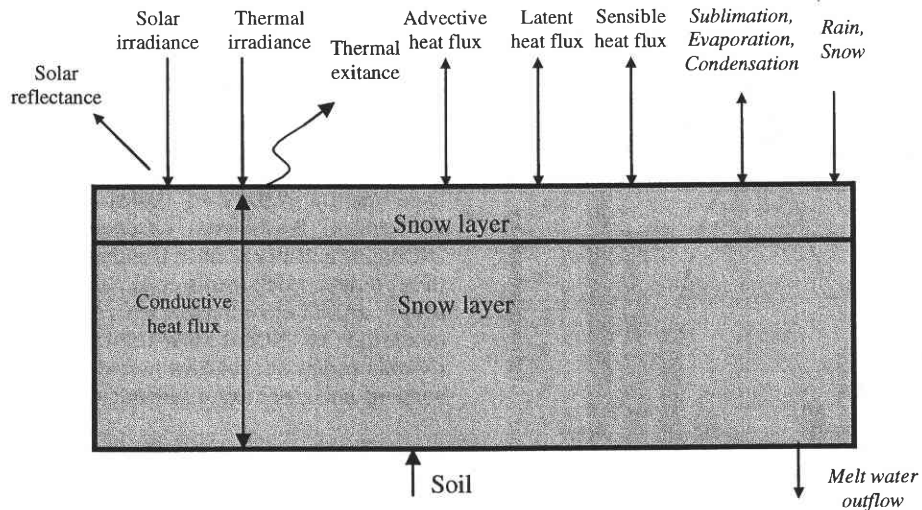


Figure 3 Conceptualization of SNOBAL (adapted from Garen and Marks, 2005).

tation, wind speed, vapor pressure and ground temperature. These forcing data were processed at 3-h intervals for model runs.

Solar

The model requires net incoming shortwave radiation data (0.3–2.8 μm), which were generated from each station's measured incoming solar radiation. In order to account for reflected shortwave radiation, a modeling approach was taken because direct measurements of albedo were not made at the study sites. The measured incoming solar radiation data was integrated over the spectral range of 0.3–2.8 μm . However, snow surface albedo varies by wavelength. The radiation data were split into two bands (visible: 0.3–0.7 μm and near-infrared (NIR): 0.7–2.8 μm) in order to apply a different albedo value to each wavelength band. The IPW utility *twostream* (Meador and Weaver, 1980) was used to estimate the fractions of incoming solar radiation for clear sky conditions in the visible (48%) and in the NIR wavelengths (52%). These fractions were applied to the measured data to determine incoming shortwave radiation in each wavelength band. A snow surface albedo model in IPW, *albedo*, was used to calculate snow surface reflectance in the visible and NIR wavelengths based on snow surface grain size growth. These albedo values were then applied to the calculated wavelength bands.

Surface deposits of debris, such as branches, needle fall and dust decrease the effective albedo of the snow surface (Hardy et al., 2000). This process plays an important role in the radiation balance of PNW snowpacks. The climate of the PNW creates snowpacks that are at or near isothermal conditions throughout the winter which results in snowmelt through the winter months. As snow depth decreases, more dust and debris concentrates at the surface, reducing the snow albedo. In order to account for changes in surface debris, a time function albedo reduction algorithm was applied:

$$\alpha_r = 0.0607 \times \ln(\text{TSS}) + 0.01398 \quad (2)$$

where TSS is the time since last snowfall. The albedo reduction (α_r) is subtracted from the calculated clean snow surface albedo. This algorithm was derived to reduce the snow albedo over a 14-day period to a lower limit of 0.6 for visible and 0.4 for NIR wavelengths, an approach similar to that of Garen and Marks (2005). The coefficients in Eq. (2) were developed by calculating a logarithmic decay for snow albedo from unity to 0.6 for the visible spectral range over the 14-day period.

This approach was evaluated and compared to other published albedo decay models, to identify discrepancies in model performance and to see the effects of different albedo modeling decay approaches on the annual snow energy budget summary. Garen and Marks (2005) applied a square root decay function with lower limits for the visible and NIR, modeled from peak snow pack to melt out. Link and Marks (1999a) used a linear decay function from peak snow pack to melt out. These two approaches were applied to the UPLMET WY1996 dataset.

Longwave radiation

Longwave (thermal) radiation (2.8–100 μm) was the only forcing parameter not measured directly at the climate stations. Longwave radiation input was estimated using a

three-step process (Garen and Marks, 2005; Susong et al., 1999). First, clear sky longwave radiation was calculated following the Brutsaert method with the IPW command *trad* (Marks and Dozier, 1979). This technique used air temperature, vapor pressure and elevation to approximate downwelling atmospheric thermal radiation during clear sky conditions. An adjustment of thermal radiation was required in order to account for incoming longwave radiation from low, dense clouds which are common during winters in the PNW. A cloud cover factor was calculated using the methodology described by Garen and Marks (2005). The IPW *twostream* (Meador and Weaver, 1980) model was used to calculate incoming shortwave radiation for afternoon clear sky measurements. The model parameters were calibrated to fit known sunny day conditions. The model was then run for the entire modeling period and compared to daily values at 1200 and 1500 Pacific Standard Time. A ratio of the modeled and measured incoming solar radiation for these time steps was then calculated to give a daily cloud coverage fraction. This ratio was incorporated into a linear regression model developed by Garen and Marks (2005), which is based on measured thermal radiation.

The sites at the HJA are located in clearings characterized as forest openings, and are subject to thermal radiation emitted by vegetation. To account for vegetation thermal radiation (L_v) an algorithm for gray body emittance was used as suggested by Link and Marks (1999b):

$$L_v = (1 - t)\varepsilon\sigma T^4 \quad (3)$$

where t is the transmissivity, ε the emissivity, σ the Stefan–Boltzmann constant and T is vegetation temperature in Kelvin. This method applies the Stefan–Boltzmann equation accounting for emissivity and transmissivity of vegetation based on field results from Link and Marks (1999b). The transmissivity of the vegetation accounts for the canopy density, the relative stand density and forest characteristics (Link and Marks, 1999b). The temperature of the vegetation was assumed to be air temperature, transmissivity of thermal radiation was assumed to be 0.75, and emissivity to be 0.96. Calculated thermal radiation from vegetation was then added to the calculated atmospheric thermal radiation. This resulted in modeled downwelling thermal radiation for SNOBAL, accounting for location, cloud cover, vegetation and atmospheric conditions.

Air temperature

Air temperature ($^{\circ}\text{C}$) was measured at 450 cm above the soil surface at each site and averaged for 3-h time steps. When data at 450 cm were missing or questionable, data from sensors at 350 cm were adjusted using a simple linear regression transfer function. Transfer functions were calculated by creating linear regressions between the 450 and 350 cm air temperature sensors at each station. WY 1999 was omitted in this analysis at VANMET because of faulty air temperature data.

Wind speed

Wind speed measurements were made at each site at 10 m above the ground surface. Average wind speeds were calculated over 3 h time periods and used in the model.

Vapor pressure

Vapor pressure is the amount of pressure exerted by water vapor molecules in a given volume of air. Relative humidity measurements were collected at each site and were used to calculate vapor pressure (Pa) and dew point ($^{\circ}\text{C}$). The calculations were carried out in IPW utilities *rh2vp* and *dewpt*.

Precipitation

Precipitation data from each site were used. Short intervals, up to 2 weeks, of missing or questionable data may have resulted from snow plugs in the precipitation gauges, datalogger failure, or undercatch. In addition to short periods of questionable data at each station, the WY 1997 record at VANMET was entirely missing. Missing values were estimated using transfer functions based on long, concurrent records at the three stations. The variability of precipitation over 3-h time periods limited the ability to develop strong correlations for short-time periods. Precipitation totals for storm events were a more accurate representation of site correlation and were used to correlate precipitation between sites.

UPLMET was chosen to fit VANMET storm totals, due to their similar elevations (Fig. 2) and known correlations of elevation and annual precipitation amounts. A transfer function for precipitation events was developed for the 8-year period. In order to have an estimate of the timing of the precipitation throughout each event, it was assumed that the fraction of the storm total for each time step which fell at UPLMET was the same at VANMET for the missing records. The assumption was then evaluated in the SNOBAL results for water year 1997.

Precipitation temperature and type were estimated using dew point temperature calculated at each site. A threshold dew point temperature of 0.5°C was used to delineate between snow and rain at VANMET and UPLMET. The threshold was determined by using SNOBAL to test threshold dew point temperatures which would most closely follow measured accumulation patterns. The 0.5°C dew point temperature threshold did not provide the proper accumulation amounts at CENMET compared to SWE measurements. Field experience has noted snow events at low elevation above 0.5°C . It was determined that a threshold dew point temperature of 1.0°C provided the proper amount of snowfall to create modeled snow accumulation patterns which fit measurements of SWE.

ROS definition

Harr and Berris (1983) defined ROS as *rain falling on a snowpack*. This simple definition does not account for negligible rainfall amounts that can fall upon the snowpack and does not produce melt or WAR. In this paper, we define ROS events at the HJA to be *eight consecutive 3-h time steps (24 h) during which rainfall is reported (≥ 0.254 mm) to fall on a snow covered surface*. This definition allows the evaluation of a number of small ROS events and to quantify their contribution to melt and WAR; whereas previous studies have focused on larger events. Adjusting the rain duration threshold (Table 2) for consecutive rainfall occurrences did not significantly affect the number of ROS events for this analysis.

Energy balance analysis

To investigate the effects of time scale analysis on the variability in the EB components, energy inputs were subdivided for WY 1996 to biweekly and event scale. WY 1996 was chosen for further analysis because of a major ROS event which occurred in February. The large ROS event of early February 1996 has been documented at other sites in the Oregon Cascade Mountains (Marks et al., 1998). This event produced flooding along the western slope of the Cascades, caused by high precipitation and melting of low-elevation snowpack. The calculated values of EB components were compared to Marks et al. (1998) to determine if modeled results for two different datasets in the same region were comparable for the same event.

Energy exchange at the soil-snow interface drives metamorphosis process in lower portions of the snowpack. The importance of this energy flux is often neglected due to the lack of soil temperature measurements. Soil temperature measurements and energy exchanges are shown to provide a basis for discussion of ground energy flux. Finally, measured and modeled SWE were used to calculate a Nash-Sutcliffe (NS) model efficiency coefficient (ME) (Nash and Sutcliffe, 1970) at each site for the periods of available snow pillow data:

$$ME = 1 - \frac{\sum_{i=1}^n (x_{\text{obs}} - x_{\text{sim}})^2}{\sum_{i=1}^n (x_{\text{obs}} - \bar{x}_{\text{obs}})^2} \quad (4)$$

where n is the number of observations, x_{obs} the observed measurement, x_{sim} the simulated and \bar{x}_{obs} is the average of the observed measurements for the modeling period.

Results

SNOBAL produced modeled energy fluxes of net radiation, ground heat, sensible heat, latent heat and advected energy. Snowpack conditions simulated include SWE, melt, snow depth, cold content, evaporation (positive and negative) and snowpack temperature. Snow pillow data were available for WY 1996–2000 at UPLMET; WY 1997–2003 for VANMET; and 1997–2003 at CENMET (Fig. 4). Only the time steps for which modeled or measured snowpack existed were included in the reported model efficiencies. The Nash-Sutcliffe efficiency for UPLMET, VANMET and CENMET were 0.94, 0.93 and 0.76, respectively. Modeled SWE matched well with measured SWE data during accumulation and melt periods at all three sites. The model had difficulties producing early season snow accumulation patterns that followed the measured data. The model has the most difficulty matching conditions at CENMET in snow years

Table 2 Number of ROS events

# of time steps	Number of ROS events for 3-h time step thresholds				
	8	7	6	5	4
UPLMET	83	99	137	171	230
VANMET	61	77	100	125	161
CENMET	56	64	94	116	149

where the snowpack accumulated and melted multiple times. The SNOBAL SWE prediction at VANMET for WY 1999 was lower than measured SWE accumulation. This is because of faulty air temperature readings at the station during that water year, which is excluded from the analysis.

Energy balance

Energy balance components at the 3 h model time step were analyzed for water years 1996–2003. Over the modeled period, net radiation was the dominant driver of snowmelt at the HJA (Fig. 5). The turbulent energy fluxes of latent and sensible heat melted considerably less snow than radiation at all sites. Turbulent energy fluxes were most important at VANMET (24% of melt). Ground heat flux contributed a surprisingly large amount of energy to the snowpack at VANMET (18%) and especially CENMET (29%) over the entire modeled period. Advected energy from rain was relatively minor at all sites (<3%).

At the annual time scale, the relative contribution of net radiation flux to snowmelt was uniformly high at UPLMET, ranging from 71% to 87%, and averaging 80% (Fig. 6). Radiation at CENMET and VANMET was also the most important driver of melt, but to a lesser degree and with higher year-to-year variability. The importance of the combined turbulent energy fluxes varied annually at each site. At UPLMET, the contribution of turbulent fluxes to the snowpack was relatively small, with little inter-annual variability (9–12%). Turbulent fluxes at CENMET and VANMET had greater variability from year-to-year. Advective heat transfer was uniformly low at all sites.

The UPLMET EB was examined at biweekly and event scales for water year 1996. The biweekly analysis showed a seasonally varying pattern of the relative importance of

the energy balance components (Fig. 7). Early-season snowmelt was driven predominantly by ground heat flux, whereas snowmelt after the peak snowpack date was generally driven by radiation.

The evaluation of alternative albedo decay models using UPLMET 1996 data produced variable SWE estimates which did not track the snow pillow data. Nash–Sutcliffe coefficients for the linear and square-root albedo reduction models are 0.87 and 0.86, while the dynamic model efficiency was 0.97. The dynamic albedo model tracked the measured SWE, following the melt rates closely at UPLMET for WY 1996.

Ground heat flux contributed a variable amount of energy to melt at each of the sites. At the annual time scale at UPLMET, ground heat flux contributions ranged from 8% to 55% for each water year. Similarly the lower elevation site, CENMET, ranged from 42% to 85% in ground energy when integrated over individual water years. These inputs reflected the positive temperatures which were measured in the soil profile (Fig. 12). Soil temperature measurements

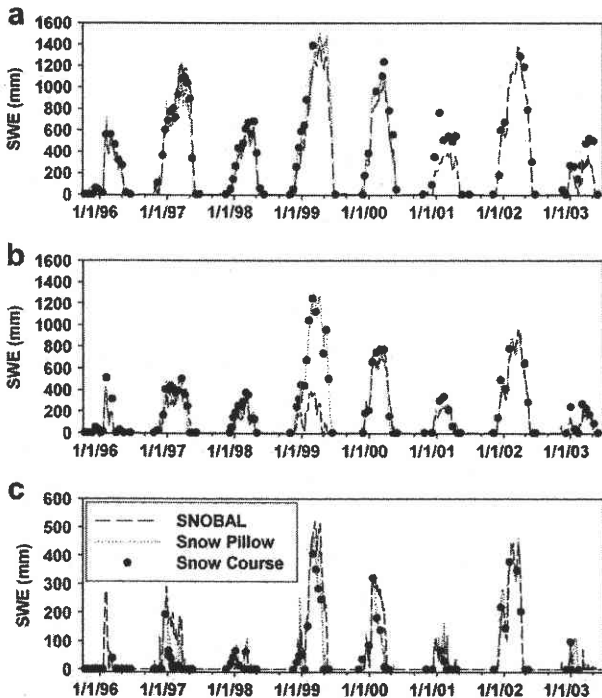


Figure 4 Modeled and measured SWE at UPLMET (a), VANMET (b) and CENMET (c).

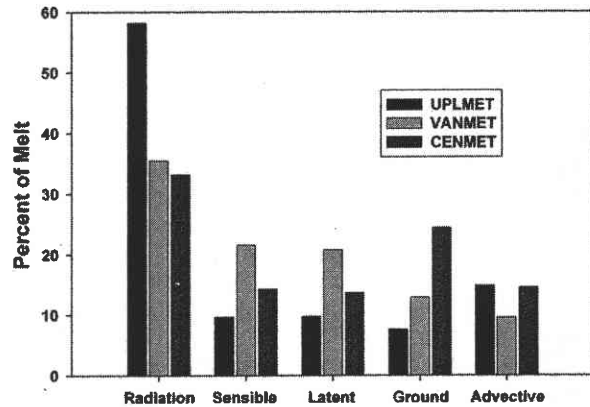


Figure 5 Modeled energy balance component contribution to total snowmelt at three sites, 1996–2003.

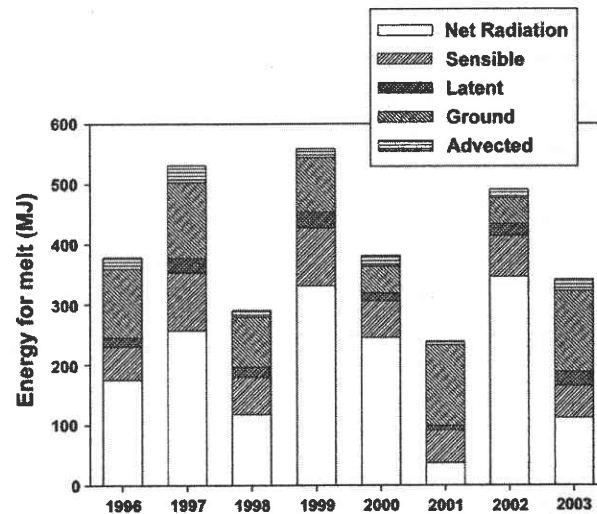


Figure 6 Annual energy balance components at UPLMET, 1996–2003.

at UPLMET did not go below freezing throughout the winter, which caused the calculated ground heat flux to be a significant portion of the energy budget.

ROS events

The UPLMET EB was examined for a major ROS event (February 1996) of 168 h at 3-h intervals (Fig. 8). Turbulent energy fluxes were important during this event, although net radiation also positively contributed to energy for snowmelt. Measured rainfall for the event was 286 mm at UPLMET, which was reflected in the high advected energy flux. As at longer time scales, the event-scale energy balance component contributions to melt varied by site for this event (Table 3); turbulent energy exchange was most important at VANMET. February 9–10 in Fig. 8 shows the typical dry-weather pattern of radiation flux alternating between night (net radiation loss from the snowpack) and day (net radiation gain).

Using our definition for a ROS event, model output at each site was separated into ROS and non-ROS periods. The number of events, precipitation amounts and melt amounts for all of these events varied by site (Table 4). The highest average ROS melt rate was observed at VANMET. However, average melt rates for ROS events did not differ substantially from non-ROS melt rates. Average energy fluxes over the ROS record for each site were calculated and are shown in Fig. 9. Net radiation flux was the dominant contributor to snowmelt during ROS events. The combination of the turbulent energy fluxes was the most important driver of melt during ROS events at VANMET, accounting for 42% of snowmelt. At CENMET, net radiation and turbulent energy exchanges were similar for ROS events. Ground heat flux contribution to melt during ROS events ranged from 8% (UPLMET) to 24% (CENMET). Advective heat transfer to the snowpack was relatively high during ROS events, ranging from 10% at VANMET to 15% at UPLMET.

The percentage of snowmelt generated during ROS events on an annual basis over the 8-year record ranged from 3% to 20% and averaged 8–12% at the three sites, while the days where ROS WAR occurred during the modeling period accounted for approximately 22% of the total days when WAR was taking place. Although total WAR produced during ROS events was often a large percentage (6–42%) of the an-

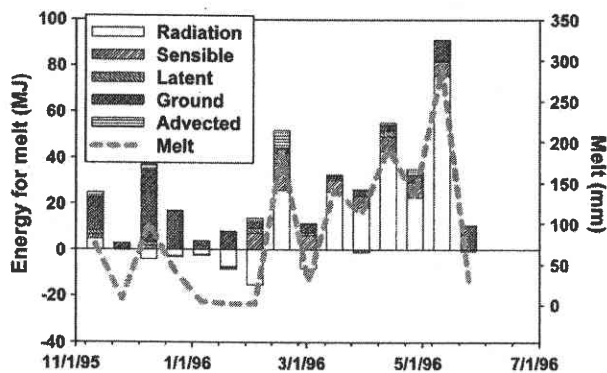


Figure 7 Energy balance components for 1996, biweekly time step.

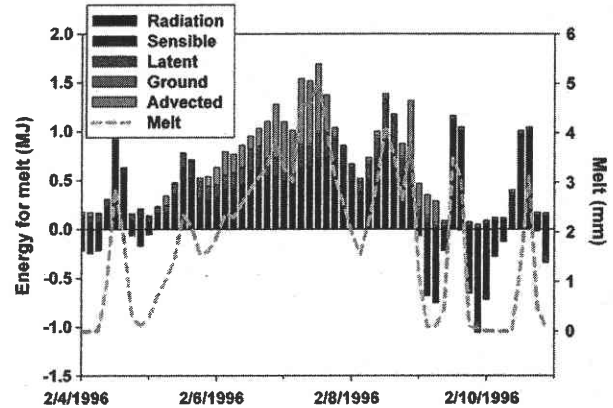


Figure 8 Energy balance components for ROS event, February 1996, 3-h time step.

Table 3 EB components for 1996 ROS event

Site	% Radiation	% Turbulent	% Ground	% Advected
UPLMET	32	38	22	7
VANMET	21	54	8	16
CENMET	29	25	23	21

nual total, WAR that occurred during ROS events was composed primarily of precipitation which percolated through the snowpack (Fig. 10). Percolating precipitation was identified as the amount of WAR less the amount snowmelt calculated. CENMET had the highest relative contribution of precipitation to WAR (annual average of 28%), and values at the two higher-elevation sites were similar. ROS events contributed the most to annual WAR at CENMET (62% for 1996) and average annual ROS (rain plus snowmelt) contribution to WAR ranged from 30% (UPLMET) to 39% (CENMET). Except for 2 years at CENMET, the majority of annual WAR was snowmelt produced by non-ROS processes.

Discussion

Energy balance variability

For the water years 1996–2003, net radiation was the dominant contributor to the energy for melt at each of the sites: UPLMET, 80%; VANMET, 55%; CENMET 49% (Fig. 5). These contributions were surprisingly high for an environment with a snowmelt regime that has been classified typically as rain-on-snow dominated (USACE, 1956). Previous work by Berris and Harr (1987) and Marks et al. (1998) has shown that tur-

Table 4 ROS events at each station

Site	Number of ROS events	Range of PPT (mm)	Average (mm)
UPLMET	83	2.4–286	52.1
VANMET	61	8.5–302	52.3
CENMET	56	4.8–321	62.5

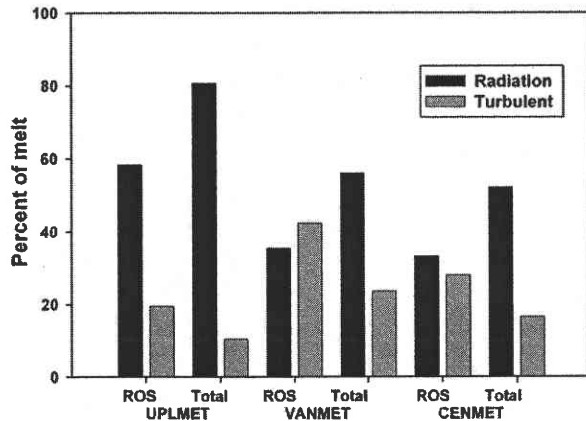


Figure 9 Modeled energy balance component contribution to snowmelt during ROS events at all three stations, 1996–2003.

bulent fluxes were important during ROS events in PNW forested environments. These energy fluxes have been assumed traditionally to be the dominant processes in the HJA which straddles the transient and seasonal snow zones and experiences numerous ROS events throughout the winter season.

The seasonal variability of net radiation contributions to melt reflected the timing of melt-out at each station. Snow that existed into late spring was exposed to longer daylight hours and more intense incoming radiation over longer periods of the day. During springtime, nighttime temperatures remained typically above freezing which supported an isothermal snowpack. The isothermal snowpack was in turn subjected to high radiation inputs during the daytime, which produced high melt rates. This resulted in high positive radiation fluxes which produced a majority of the annual snowmelt. Conversely, shallow snowpacks melted out earlier in the season and were therefore exposed to fewer high net-radiation flux days.

Over the 8-year record, snow melted out sooner at VANMET than at UPLMET. The UPLMET and VANMET sites were at a similar elevation, but nearly opposite aspects. VANMET faced south, and was therefore exposed to the prevailing winds during winter and spring storms, whereas UPLMET's north aspect provided shelter from prevailing winds and incident solar radiation. Accordingly, turbulent energy fluxes were higher at VANMET than at UPLMET. Although VANMET was more exposed to direct-beam solar radiation than UPLMET, radiation was a more important driver of annual snowmelt at UPLMET. This was due to the late season snowpack at UPLMET which was subject to high solar insolation during the late spring.

The CENMET site is 300 m lower in elevation than UPLMET and VANMET, with a southeast aspect. Measured air temperatures were higher than the other study sites, resulting in much lower annual snowfall. The lower snow accumulation tended to melt quickly and was not exposed to late spring high solar insolation days. Shallow snow accumulations in early winter were subject to warm ground temperatures, which caused fast melt out, and was reflected in high ground heat flux during low snow years.

When EB components for the accumulation and melt season were quantified separately, it became clear that during

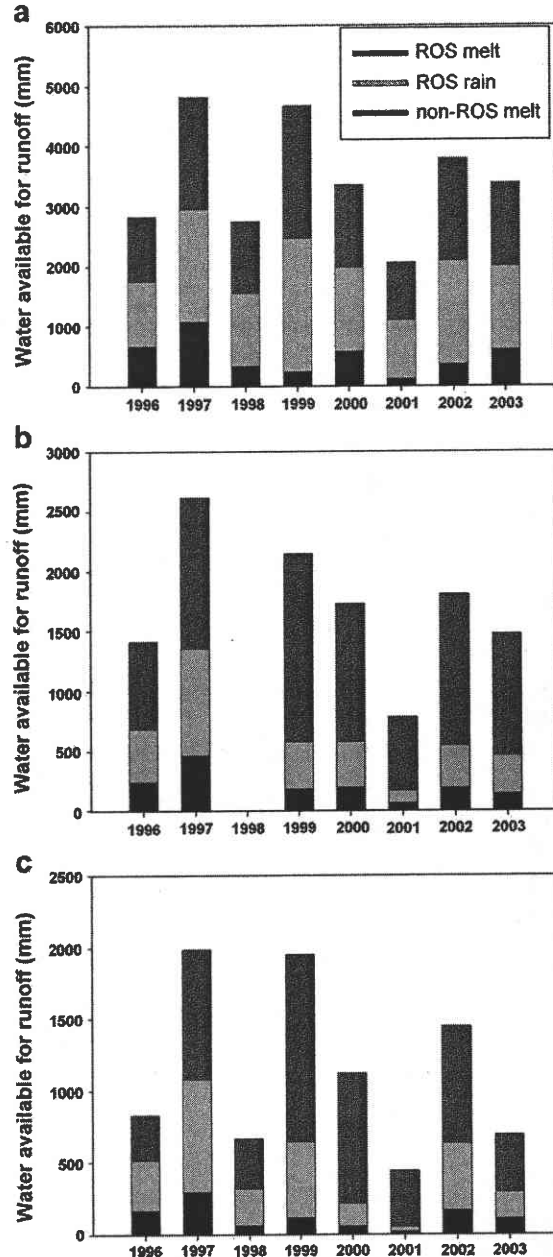


Figure 10 Water available for runoff derived from ROS events (rain + snowmelt) and non-ROS periods (snowmelt only) at UPLMET (a), VANMET (b) and CENMET (c).

early to mid-winter, relatively little snow melted, especially at the upper sites. Melt that occurred during this period was driven mainly by ground heat flux. Ground temperatures were typically above 0 °C, with temperatures well above freezing throughout the fall and prior to snowfall. Consequently, shallow, early-season snow tended to melt quickly. As the snowpack accumulated, ground temperature remained steady at temperatures just above freezing. The snowpack generally showed a loss of net radiation as a consequence of shorter days and generally cloudy weather. These conditions limited incoming shortwave energy, while high snow surface albedo reflected a large pro-

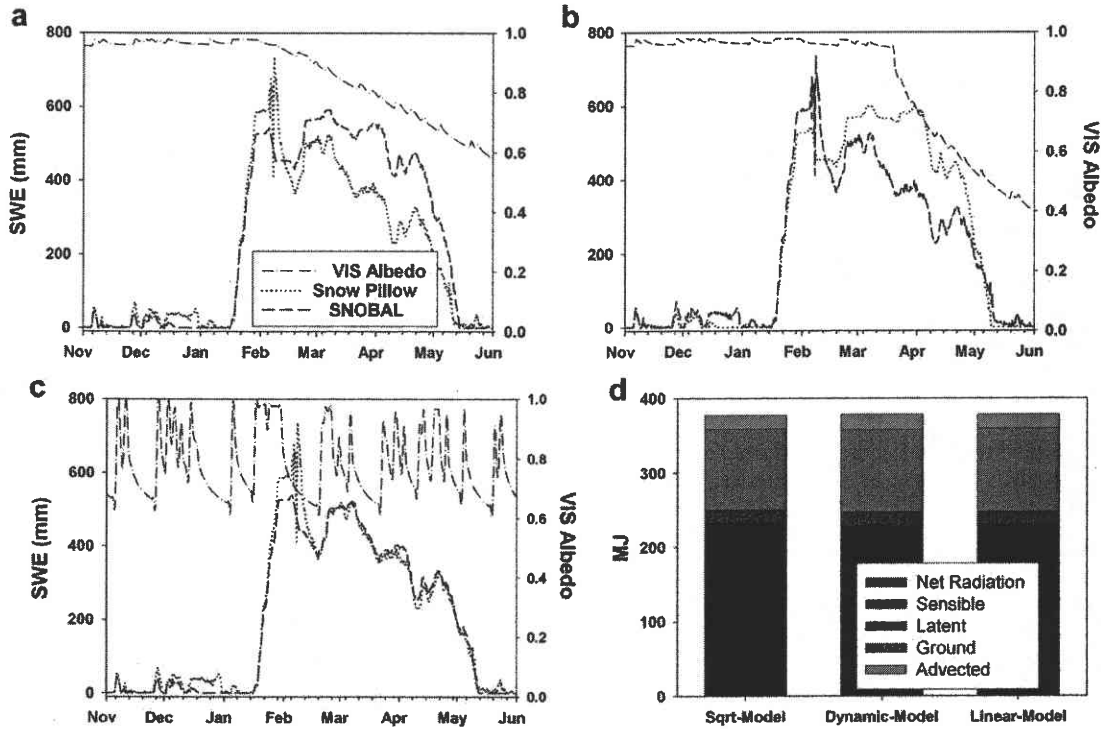


Figure 11 Energy balance components for WY 1996 for each albedo-reduction algorithm – linear decay (a), square root (b), dynamic (c) and annual EB for each function (d).

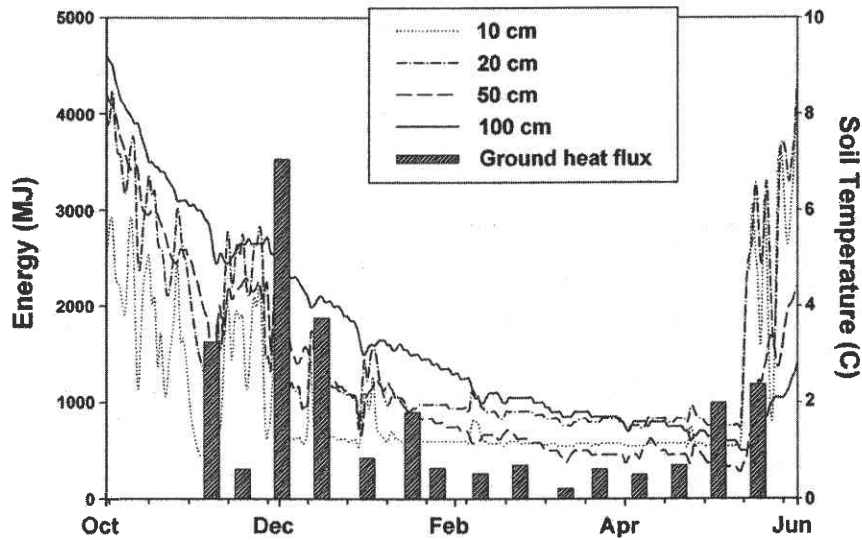


Figure 12 Soil temperatures at depth and ground heat flux for WY 1996. Note the high ground heat flux in December, due to numerous snow events where accumulation was on bare ground with relatively warm temperatures.

portion of the radiation which did reach the snowpack. Turbulent fluxes were positive throughout the winter period but low, due to low temperature and vapor pressure gradients and generally low wind speeds.

Evaluating net solar radiation modeling

Net solar radiation (0.3–2.8 μm) inputs to the snowpack are controlled by atmospheric conditions, solar angle,

duration of daylight hours and albedo. Incoming solar radiation to the atmosphere and the effects of solar angle and topography are generally well understood in the literature (Dozier, 1980; Marks et al., 1992), our understanding of snow surface albedo in forested catchments for modeling applications is still limited. Clean snow albedo has been well correlated with snow surface and grain size (Wiscombe and Warren, 1980). Although the process of grain size growth can be estimated over time (Marks et al.,

1999b), the effects of vegetation and atmospheric deposition of debris on the snow surface is poorly understood. Recent modeling approaches (Garen and Marks, 2005; Link and Marks, 1999a) have accounted for the increased snow surface debris by applying simple decay functions from peak snowpack to melt out. Although these approaches resulted in good model fits, measurements of SWE are required at the site to apply the albedo reduction model. This technique is unsuitable for modeling areas with no or limited measurements, as is often the case with SWE. In contrast to other approaches, our model relies on a continuous deposition of litter and atmospheric debris on the snow surface (common in forested regions), and not on timing of peak snow pack to melt out. This time decay function technique was effective for this modeling of the snowpack in the PNW forest, because of the near-isothermal snowpack conditions. The relatively warm snowpack was subject to small melt events throughout the snow season, allowing debris to accumulate at the snow surface, which reduced the snow surface albedo (see Fig. 11).

Evaluating ground heat flux

Ground heat flux is often thought of as negligible in snow energy budgets (Male and Gray, 1981). This has led to many distributed modeling approaches to assume a ground temperature of 0°C. Our EB results contradicted this assumption. The results showed that integrating the contribution of ground heat flux over annual time scales resulted in a significant positive energy flux from the ground to the snow pack. This positive energy exchange was modeled to be high when early season snow fell on a snow free ground surface. Fig. 12 shows increased ground heat flux during December, while there were numerous small snow accumulations on a snow free ground surface. This modeled energy exchange of early season and small accumulation melt on bare ground results in high annual ground heat flux values. Positive ground temperatures were often measured beneath the snowpack, which caused small amounts of melt throughout the winter, contributing to snowpack metamorphism. While the high measured ground temperatures resulted in increased overall modeled melt rates, one confounding issue is that the snow pillows have been shown to influence ground heat flux (Johnson and Schaefer, 2002). This may result in some discrepancies because bare ground conditions are simulated by SNOBAL.

Mid-winter contributions of ground heat flux were minor in our evaluation of UPLMET data at a biweekly time step (Fig. 7). Measured soil temperatures at multiple depths (Fig. 12) showed soil temperatures throughout the snow season were above 0°C. Fluctuations in temperature reflected melt water pulses through the soil profile. Some bias from the soil temperature measurements may have over estimated ground energy flux. The temperature measurements should have been essentially 0°C during spring melt when water percolated through the soil profile. The uncertainty of this energy contribution rested within the calculation of effective heat transfer from the soil to the snow. The calculation within the model (Marks et al., 1998) relied on thermal conductivity measurements of bare mineral soils, which may not have portrayed the conditions that exist in the HJA.

Rain-on-snow

1996 event

During the February 1996 ROS event, melt rates and energy balance components were influenced by high wind speeds with warm, moist air. This created conditions for high turbulent energy fluxes and added moisture to the snowpack through condensation. Model calculations also showed a net gain of radiation throughout the event. Net shortwave radiation inputs were low due to clouds, while the warm temperatures and high humidity increased the incoming thermal radiation from the low cloud cover. Turbulent fluxes were not calculated to be as high as in Marks et al. (1998), due to lower wind speeds measured at UPLMET compared to locations elsewhere in the Cascades used by Marks et al. (1998). The calculated advected heat fluxes were higher than those values reported Marks et al. (1998) in their analysis of EB during the February 1996 event. While dew point temperature was used as a proxy of precipitation temperature in both studies our reported higher advected fluxes may have been due to higher local temperature at the HJA sites than at the Marks et al. (1998) sites. Local topographic features may have allowed warmer low elevation air to be pushed up the basin and trapped, causing warmer local temperatures and higher dew point temperatures.

High-frequency ROS events

One focus of snowmelt-process research in the PNW has been ROS events (Harr, 1981; Berris and Harr, 1987; Marks et al., 1998, 2001). These studies have shown that peak-flow events in the transient and transitional snow zone are often characterized by shallow snow at low elevations and high rainfall amounts coupled with high wind speeds. WAR is produced by two main processes: melt from within the snowpack and percolation of rainfall through the snowpack (Singh et al., 1997). Shallow snowpacks and preferential flowpaths allow for shorter travel time of the rainfall through the pack and into the soil. In addition to the percolation of rainfall, water is added to the snowpack through condensation. Condensation adds water and releases energy into the snowpack, contributing to the net energy available to melt snow. This process requires high turbulent exchanges rates controlled by wind speeds. Marks et al. (1998) showed that forested areas have much lower turbulent exchanges due to lower wind speeds.

Field and modeling approaches have extended our knowledge of the melt processes which dominant ROS events. Large events, such as the February 1996 event, resulted in regional flooding due to high amounts of rain on a low elevation snowpack, warm temperatures and high wind speeds. Events of this magnitude are uncommon in the PNW. In the 8-year HJA dataset, we identified 83 ROS events at an upper elevation site (UPLMET) and 56 events at a lower elevation site (CENMET). The longer-duration snowpack at the higher-elevation site was exposed to more rain events over the course of the snow seasons. The highest event rainfall amount at each site was the February 1996 event (Table 4).

Our analysis of ROS events for the entire model period showed that radiation dominated the EB during ROS melt at UPLMET (Fig. 9). This site was protected from the prevailing wind direction during storm events, which resulted in lower turbulent-exchange rates. The deeper snowpack,